Advanced Fluid Dynamics Final Exam: Algebraic stability analysis of a base flow evolving over the suction side of a turbine blade profile

Roberto Guida Luca Baggetta

Abstract

The aim of this work is to provide a linear stability analysis of a real flow evolving over low pressure turbine blade profile and measured through a PIV system. An eight order polynomial function is adopted to fit the experimental data in the boundary layer. The resulting base flow is introduced in the Orr Sommerfeld Squire system. Eigenvalues and eigenvectors of the OSS system for the temporal problem are determined so that the less stable eigenvalue growth rate is converted into a spatial growth rate using the Gaster's transformation. The evolution of the perturbation growth rate along the streamwise direction is presented and discussed. The limits of using the Gaster's transformation and of considering a perturbations algebraic growth mechanism for the present base flow are discussed.

1 Introduction

The prediction of the boundary layer transition is a key information for evaluating the aerodynamic efficiency of low pressure turbine (LPT) blades for aeroengine application. An early transition, driven for instance by high values of the free stream turbulence (FSTI), could avoid the laminar separation which may occur due to the strong adverse pressure gradient that affects the latter part of the suction side.

The linear stability theory represents an useful tool for studying the evolution of small disturbances in flows which undergo a transition from laminar to turbulent state. Indeed, it is expected that whenever the amplitude of such small disturbances grows the flow is unstable and transition may occurs. Such unstable disturbances are known as Tollmien-Schlicting waves and took the name from the first authors who identified them. One may use the growth rate of the amplitude of these disturbances to identify the conditions that lead to the maximum amplification of the disturbance's energy and set the onset of transition where this maximum occurs. This is the principle of the the well known e^N method (see Arnal 1994). The factor N, defined as $N(x) = ln(A(x)/A_0)$, is introduced, where A_0 is the initial amplitude of the disturbance and $A(x)$ is the amplitude at a datum streamwise position. Comparison with experimental transition data (Smith and Gamberoni 1956 for instance) collected for a Blasius boundary layer, had shown that N is nearly constant (between 7 and 9) at the measured transition point. This means that the breakdown to turbulence occurs when the amplitude of the unstable Tollmien-Schictling waves becomes 7-9 times larger than the initial amplitude.

It is argued that the e^N method is as simple to use as hard to be applied to the boundary layers that occur on turbine blades. In this case the free-stream turbulence intensity as well as the pressure gradients affect the transition process which likely occurs through the by-pass mechanism defined by Morkovin (1969). Modifications of the e^N method were proposed to account for the free-stream turbulence which acts reducing the value of N at transition. Andersson et al (1999) made an attempt at prediction of bypass transition, due to algebraic mode, by correlating the transition Reynolds number and the free-stream turbulence level.

In the present work the PIV measured boundary layer evolving on the rear part of the suction side of a LPT blade, characterized by strong adverse pressure gradient, is presented. The velocity profiles that occur in any streamwise position have been reduced and analyzed through the linear stability theory by calculating the eigenvalues and eigenvectors of the Orr-Sommerfeld-Squire operator for the current base flow. The stability properties of the base flow as function of the streamwise-position (local Reynolds number and base flow variations) and the directional wavenumbers are presented and discussed.

2 Governing Equations

2.1 The Orr-Sommerfeld and Squire Equations

The governing equation for small disturbances evolving in a parallel viscous mean flow $U(y)$ obtained from the linearized Navier-Stokes equations, can be reduced into the following pair for the normal velocity v and vorticity η:

$$[(\frac{\partial}{\partial t}+U\frac{\partial}{\partial x})\nabla^2 - U''\frac{\partial}{\partial x} - Re^{-1}\nabla^4]v = 0 \quad (1)$$

$$[\frac{\partial}{\partial t}+U\frac{\partial}{\partial x} - Re^{-1}\nabla^2]\eta = -U'\frac{\partial v}{\partial z} \quad (2)$$

where the prime denotes derivation with respect to y. The Reynolds number is defined as $Re = U_\infty \delta/\nu$ where δ is the boundary layer thickness. The stability of the base flow is studied with respect to wave-like perturbations. Thus the disturbances are assumed of the form:

$$v(x,y,z,t) = \tilde{v}(y)e^{i(\alpha x+\beta z+\omega t)} \quad (3)$$

$$\eta(x,y,z,t) = \tilde{\eta}(y)e^{i(\alpha x+\beta z+\omega t)} \quad (4)$$

where α and β denote the streamwise and spanwise wave numbers respectively while ω stands for the frequency. The Orr Sommerfeld and Squire equation are therefore obtained:

$$[(-i\omega + i\alpha U)(D^2-k^2) - i\alpha U'' - Re^{-1}(D^2-k^2)^2]\tilde{v} = 0 \quad (5)$$

$$[(-i\omega + i\alpha U) - Re^{-1}(D^2-k^2)]\tilde{\eta} = i\beta U'\tilde{v} \quad (6)$$

with the boundary conditions $\tilde{v} = D\tilde{v} = \tilde{\eta} = 0$ at solid walls and in the free-stream. D and prime denote derivation with respect to y, $k^2 = \alpha^2+\beta^2$.

In the present work the temporal problem is considered for the wavelike perturbation, thus the frequency ω is a complex value while α and β are real. The frequency can then be written as $\omega = \omega_r + i\omega_c$ where ω_i represents the growth rate of the disturbance amplitude. Alternatively, the phase speed $c \in C$ is considered, where $c = c_r + ic_i = \omega/\alpha$.

The two equations can be written in matrix form which is more suitable for the solution of the eigenvalue problem other than presented in a compact notation. The composite state vector $\tilde{q}$ is introduced, which consists of the normal velocity and normal vorticity $\tilde{q} = (\tilde{v}, \tilde{\eta})^T$. Therefore, the Orr-Sommerfeld and Squire equations 5 and 6 can be written in the following form:

$$-i\omega \begin{bmatrix} k^2-D^2 & 0 \\ 0 & 1 \end{bmatrix} \begin{pmatrix} \tilde{v} \\ \tilde{\eta} \end{pmatrix} + \begin{bmatrix} L_{OS} & 0 \\ i\beta U' & L_{SQ} \end{bmatrix} \begin{pmatrix} \tilde{v} \\ \tilde{\eta} \end{pmatrix} = 0 \quad (7)$$

with:

$$L_{OS} = 1\alpha U(k^2+D^2) + i\alpha U'' + Re^{-1}(k^2+D^2) \quad (8)$$

$$L_{SQ} = 1\alpha U + Re^{-1}(k^2+D^2) \quad (9)$$

Finally, the eigenvalue problem is written with compact notation and becomes:

$$\mathbf{M}^{-1}\mathbf{L}\tilde{\mathbf{q}} = i\omega\tilde{\mathbf{q}} \quad (10)$$

where the matrices $\mathbf{M}^{-1}$ and $\mathbf{L}$ are:

$$\begin{bmatrix} k^2-D^2 & 0 \\ 0 & 1 \end{bmatrix} \quad (11)$$

$$\begin{bmatrix} L_{OS} & 0 \\ i\beta U' & L_{SQ} \end{bmatrix} \quad (12)$$

2.2 The Gaster's transformation

The evolution of the amplitude of a disturbance growing within a boundary layer represents a spatial problem rather than a temporal one. The governing equations still remain in the general form of equations 5 and 6, while the phase velocity c is a real quantity and α is defined complex. The imaginary part α_i represents the spatial growth rate of the disturbance. Thus, the spatial stability problem consists of solving the spatial wavenumber α which constitutes an eigenvalue problem where the eigenvalue appears nonlinearly with increasing matematical efforts.

Gaster (in Gaster 1962) proposed a transformation to convert the growth rate of the temporal problem into spatial growth rates. It is assumed that the perturbation velocity for the hydrodynamic linear stability problem is given by equations 3 and 4. The characteristic function relating the eigenvalues α and ω at a given Reynolds number is:

$$F(\alpha,\omega) = 0 \quad (13)$$

The temporal case is labeled (T) with $\alpha_i(T) = 0$ and $\alpha = \alpha_r(T)$, $\omega = \omega_r(T) + i\omega_i(T)$, while the spatial case, labeled (S), is characterized by $\omega = \omega_r(S)$ and $\alpha = \alpha_r(S) + i\alpha i(S)$. Then, it is considered that spatial and temporally growing modes belong to a region where ω is an analytic function of α. With this assumption the Cauchy-Riemann relations are:

$$\frac{\partial \omega_r}{\partial \alpha_r} = \frac{\partial \omega_i}{\partial \alpha_i} \quad (14)$$

$$\frac{\partial \omega_r}{\partial \alpha_i} = -\frac{\partial \omega_i}{\partial \alpha_r} \quad (15)$$

These relations are integrated with respect to α_i from state (T) to state (S) keeping $\alpha_r = \alpha_r(T) = cost$ and under the hypothesis that the growth rates are small. The following

relation is obtained:

$$\frac{\omega_i(T)}{\alpha_i(S)} = -\frac{\partial \omega_r}{\partial \alpha_r} \tag{16}$$

which relates the spatial growth rate α_i to the temporally growth rate ω_i through the group velocity $c_r = \partial\omega_r/\partial\alpha_r$. It is worth noting that the previous relation results from considerations of mathematical nature and the only assumption of small growth rate is made. Thus the relation is valid only in the neighborhood of the neutral curve where $\omega_i \approx 0$. In the present work the eigenmode and eigenvectors of the OSS system are determined for the temporal case, then the spatial growth rate α_i is obtained from the less stable eigenmode $max(c_i)$ of the discrete spectrum, using the relation 16.

3 Test facility and data reduction

3.1 Experimental apparatus

The experimental investigations have been performed in a 7-blade large-scale planar cascade, representative of highly loaded LPT blade profiles, feed by a blow-down wind tunnel. The blades are characterized by a chord of 120 mm and an aspect ratio $AR = 2.5$ to ensure two-dimensional time-mean flow at midspan. Measurements have been carried out at a low Reynolds number condition $Re = 70000$ (defined on the blade chord and the isentropic exit velocity) with a free-stream turbulence intensity of $FSTI = 5.2\%$. In order to characterize in detail the dynamics leading to the transition process of the suction side boundary layer, PIV measurements have been performed in the wall-normal plane as shown in figure 1. The PIV field of view of the wall-normal plane extends from $s/s_{max} = 0.74$ to the blade trailing edge and from the wall up to $y/g = 0.1$ in the streamwise and wall-normal directions respectively (with s_{max} the suction side surface length and g the cascade pitch).

The PIV instrumentation is constituted by a double-cavity Nd: Yag pulsed laser BLUESKY-QUANTEL CFR200 (energy 2x100 mJ per pulse at 532 nm, pulse duration 8 ns, repetition rate 10 Hz). The optical system forms a light sheet of 1 mm thickness. The light scattered by the seeding particles mineral oil droplets with a mean diameter of 1.5 μm) is recorded on a high sensitive digital camera with a cooled CCD matrix of 1280 x 1024 pixels (with single pixel dimension of 6.7x6.7 μm^2). The camera maximum frame rate in the double frame mode is 4.5 Hz, and the minimum frame interval is 200 ns. The magnification factor for the present experiments was set to $M = 0.165$. The cross-correlation function has been calculated on a 16x16 pixels interrogation area with a 50% overlap. This corresponds to a spatial resolution of $0.325x0.325\ mm^2$. The instantaneous velocities have been estimated with an accuracy of 3.0%.

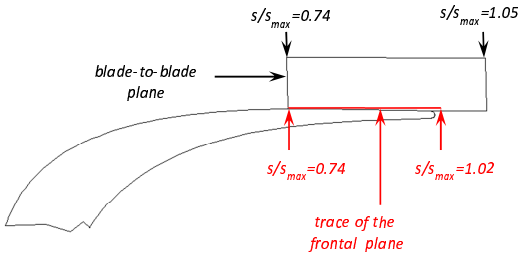

Figure 1: Measuring domain over the suction side of the blade profile

3.2 Polynomial fit

The measured domain is constituted by 159 and 30 points in the streamwise direction and y direction respectively. The boundary layer is described by 6 up to 12 points along the y direction in the different streamwise positions. In order to make the measured boundary layer profile suitable for a linear stability analysis, the experimental data have been reduced through a polynomial fit. In this way the number of velocity values describing the boundary layer can be set to the needed value (equal to the modes number) and the first and second derivative of the non-dimensional velocity U are directly calculated.

The fitting process is performed on the points along the y direction from the wall (where the no slip condition $U(y = 0)$=0 has been added artificially) up to the first measured point out of the boundary layer thickness δ. The velocity values out of the boundary layer are constant along y and equal to the local external velocity thus $U(y \geq \delta) = 1$, so that $\partial U/\partial y$=$\partial^2 U/\partial^2 y$=0 for $y > \delta$. An eight order polynomial has been adopted. Figure 2 shows the comparison between the experimental data for a fixed streamwise position and the polynomial resulting from the fitting as well as the first and second derivative of the fitted velocity using 400 points. The agreement between the polynomial and the experimental data is good within the boundary layer thickness while a slight difference can be noticed in the outer part of the domain.

The OSS eigenvalue problem has been solved for the base flow presented in the previous figure 2 as validation of the fitting process. There were considered the wavenumbers $\alpha = 0.4$ and $\beta = 0.4$. The y coordinate is discretized using Chebyshev-spectral technique with 400 points. Figure 3 shows the eigenvalues of the OSS equation for the present example. It can be noticed that the structure of the spectra is similar to the eigenspectra of the Blasius boundary layer (see Schmid and Henningson

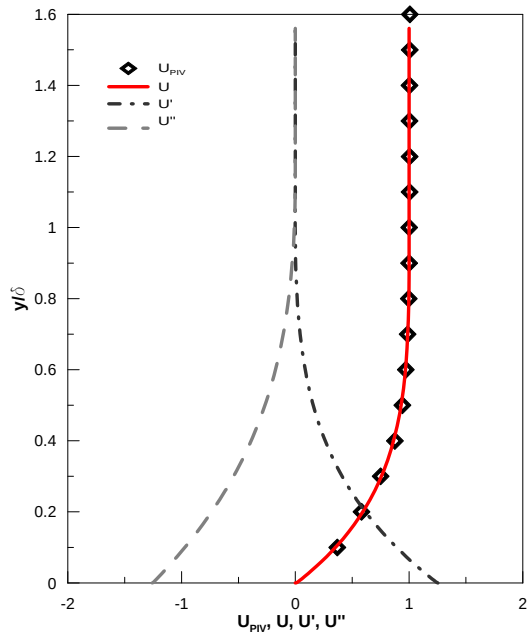

Figure 2: Comparison between experimental data and polynomial fitting of the streamwise mean velocity, and behaviour of first and second derivative of the polynomial function.

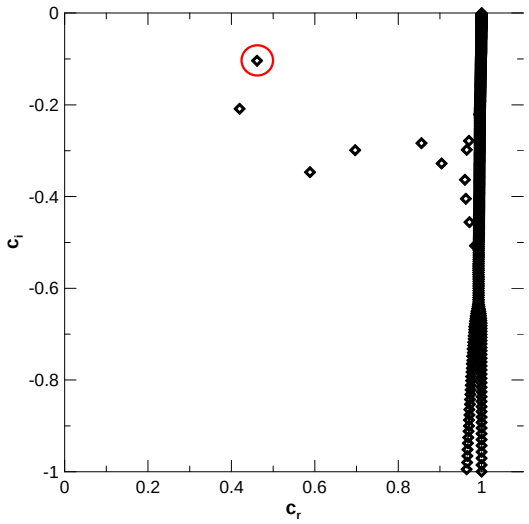

Figure 3: Spectrum for boundary layer flow presented in figure 2 forα=0.4, *Re*=375

2012). The points close to the abscissa $c_r = 1$ constitute the so-called continuous spectrum while the discrete spectrum is constituted by the modes on the left branch of the continuous spectrum. It is demonstrated that the boundary layer has at most one unstable eigenmode, denoted Tollmien-Schittling wave, which appears always on the discrete spectrum. It is the less stable eigenvalue of the discrete spectrum highlighted by the red round in figure 3. For the parameter combination shown in the present case, the Tollmien-Schittling mode is stable. The corresponding eigenfunctions $\tilde{u}$ and $\tilde{v}$ are plotted in figure 4 which also appear similar to the ones computed for the Blasius boundary layer.

3.3 Modes number sensitivity

The sensitivity of the eigensolution of the the Orr-Sommerfeld-Squire system with respect to the number of modes has been analyzed. The eigenvalue problem of eq. 10 has been solved for the base flows corresponding to the streamwie positions s/s_{max} = 0.9 and 0.95. Different values of mode number parameter n are considered, from 111 up to 1000, and also the wave-number α is varied from 1 up to 1.4 while $\beta = 0$ in both cases. The dependency of the spatial growth rate upon the mode number parameter n is shown in figures 5.

It can be observed that the solution (in terms of α_i) does not depends on n for n higher than 200 for every α, β and base flow conditions. The following results have been therefore obtained using $n = 400$ which appears the best choice in terms of accuracy of the solution and computational efforts.

4 Results

4.1 PIV mean results

Figure 6 reports the spatial distribution of time mean streamwise velocity and rms of velocity fluctuations normalized by the free-stream velocity (U_0) at the measuring domain inlet. The time-mean values $\overline{u}/U_0$ indicates an attached boundary layer growing through the latter part of the blade and beyond the trailing edge where the flow is unbounded. Large values of unresolved unsteadiness can be observed at the measuring plane inlet. They progressively increase up to $s/s_{max} = 0.98$, where the contour plots show the maximum values. Previous works (i.e. Lengani and Simoni 2015) indicates that the boundary layer may be considered transitional in the region beyond $s/s_{max} = 0.85$.

4.2 Modal analysis

The experimental streamwise mean velocity has been fitted through the way described previously and the OSS eigenvalue problem has been solved for every streamwise base flow. Then the less stable eigenvalue of the discrete spectrum is identified and the spatially growth rate α_i is

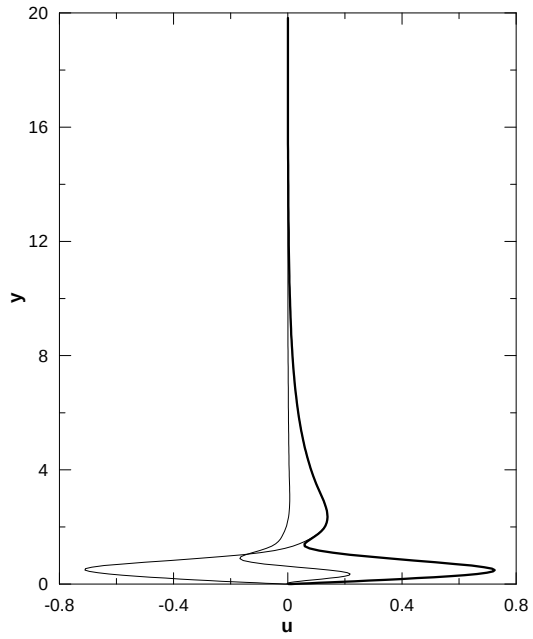

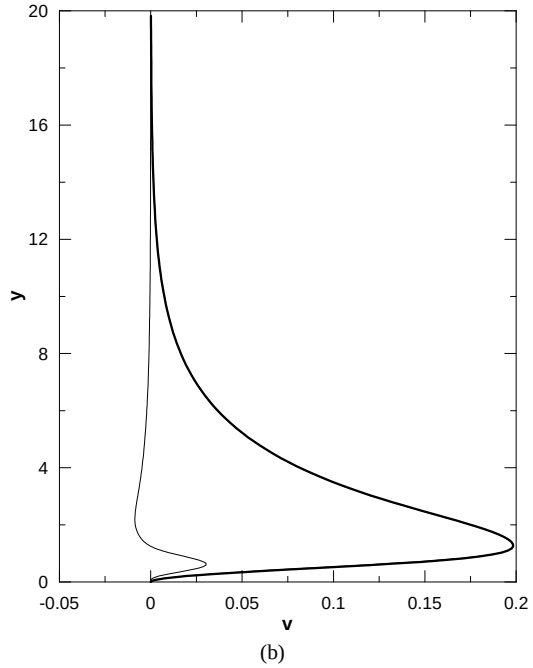

Figure 4: Eigenfunctions of u (a) and v (b) of the less stable eigenvalue in figure 3, Thick lines represents the absolute value, the thin lines are the imaginary and real part

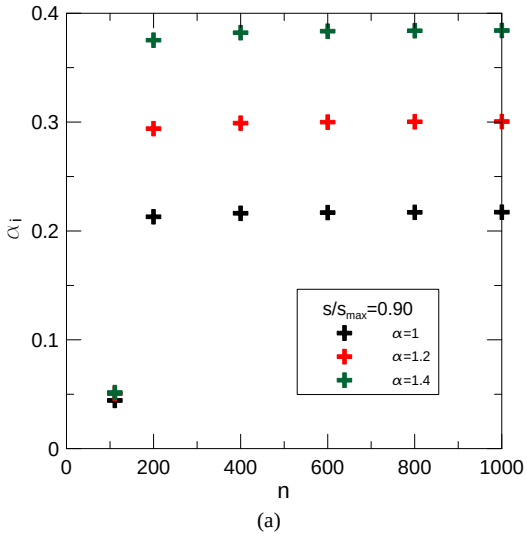

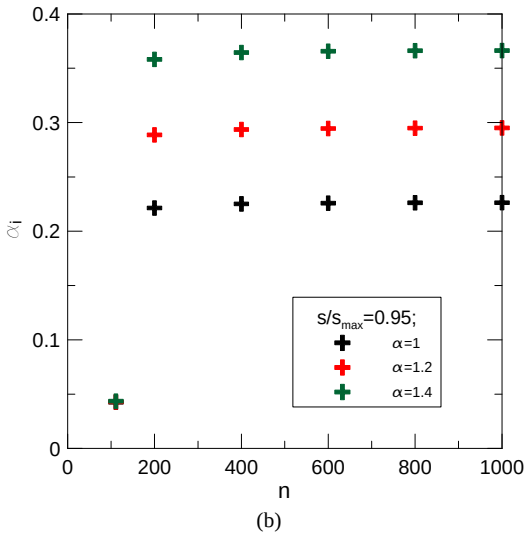

Figure 5: α_i dependency upon the mode number n and wavenumber α

derived from eq. 16. The analysis is provided for a wide range of wavenumbers α and β while the Reynolds number depends on the local flow properties.

The behavior of α_i as function of the non-dimensional streamwise coordinate is plotted in figure 7. Particularly figure 7a shows different curves corresponding to the solutions for $\beta = 0$ and different values of α while figure 7b provides the effects of $\beta > 0$. Evidence of an algebraic stability of the flow emerges from the previous figures for $\alpha_i(x) > 0$ in every positions. The discordance with the experiments that reveal a boundary layer transition, thus instability of the flow, will be discussed later.

For the case of $\beta = 0$ (figure 7a) the less stable condition is obtain for $\alpha = 0.05$ and $s/s_{max} < 0.87$. Then the curve of $\alpha = 0.4$ becomes lower and a minimum value is reached in correspondence of $s/s_{max} < 0.9$. It further rises and becomes higher than $\alpha = 0.05$ downstream of $s/s_{max} = 0.9$.

The introduction of the Squire modes, i.e. positive val-

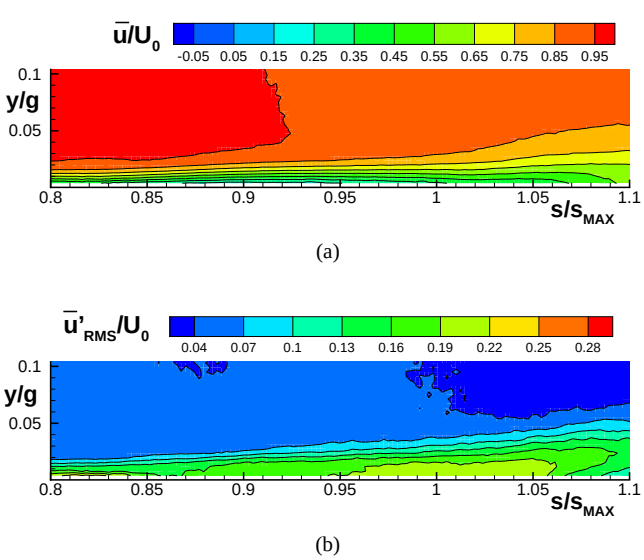

Figure 6: Distribution of the mean streamwise velocity component (top) and rms of the streamwise velocity fluctuations (bottom)

ues of β, increase the stability for the conditions $\alpha = 0.4$ and 1.1 but acts in the opposite way for the lowest α. This is in contrast with the Squire's theorem enunciating that Squire modes are always damped.

In order to better investigate this trend, the contour plots of α_i as function of α and β for s/s_{max} = 0.9 and 0.95, are plotted in figure 8.

In figure 8a a minimum value of α_i is observed in (α, β) = (0.38, 0). It increases as the two wavenumbers become higher. A different behavior is observed in figure 8b where the minimum value for α_i is obtained for α close to zero ($\alpha = 0$ cannot be investigated) and $\beta = 0.4$.

Therefore, the results for the temporal problem need to be presented and discussed. Figure 9 shows the contour plot of the temporally growth rate of the less stable eigenvalue c_i for the same positions presented in figure .

The curves of constant grow rate again resemble the ones for Blasius boundary layer (see Schmid and Henningson 2012). Both cases are stable and the less stable condition is reached in both positions for $\beta = 0$ and α close to 0.38. As α approaches zero c_i becomes drastically lower and thus moves away from the condition $c_i = 0$ corresponding to the neutral curve and to the region of validity of the Gaster's transformation. It follows that the results in terms of α_i can be considered valid only in the range of α and β that lead to c_i close to 0. Thus for $0.27 < \alpha < 0.42$ and $\beta < 0.2$.

Nevertheless, the streamwise evolution of α_i for the condition (α, β) = (0.4, 0) shown in figure 7 indicates that the flow becomes less stable as it approach the position where the transition occurs according to experimental data (approximately $s/s_{max} = 0.85$) but it never becomes unstable. Thus the evolution of the small disturbances can not be describe through an algebraic growing mechanism. Measurements in the wall-parallel plane (presented in Lengani and Simoni 2015) reveals the presence of streamwise elongated flow patterns with alternating low and high momentum. The formation of those streaks have been identified has the consequence of a non-modal disturbance growing mechanism and their breakdown leads to the so called by-pass transition mode.

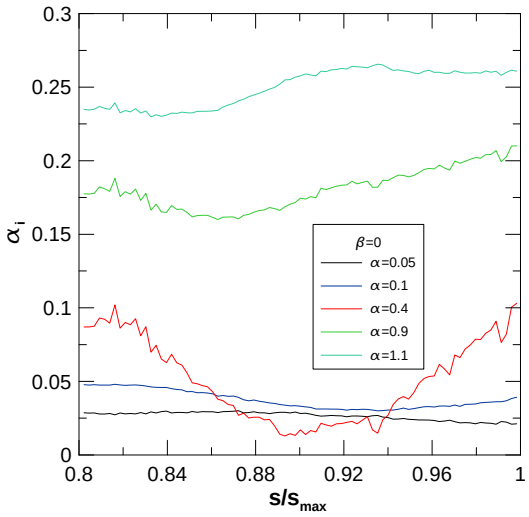

Figure 7: Evolution of the growth rate α_i along the nondimensional streamwise coordinate

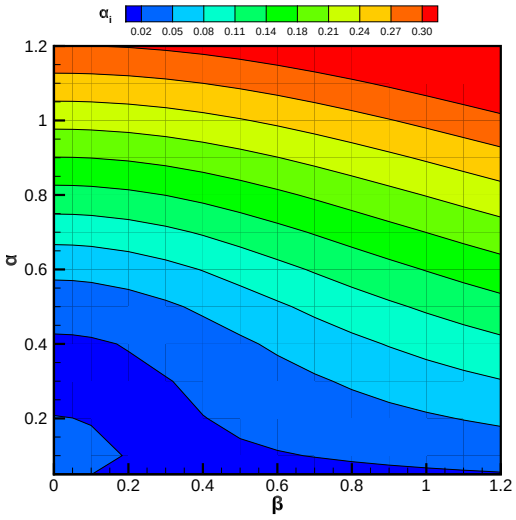

(a)

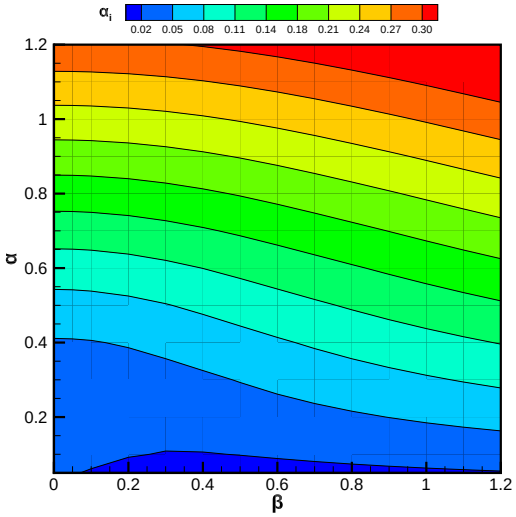

(b)

Figure 8: Contour plots of the spatial growth rate α_i for $s/s_{max} = 0.9$ (top) and $s/s_{max} = 0.95$ (bottom)

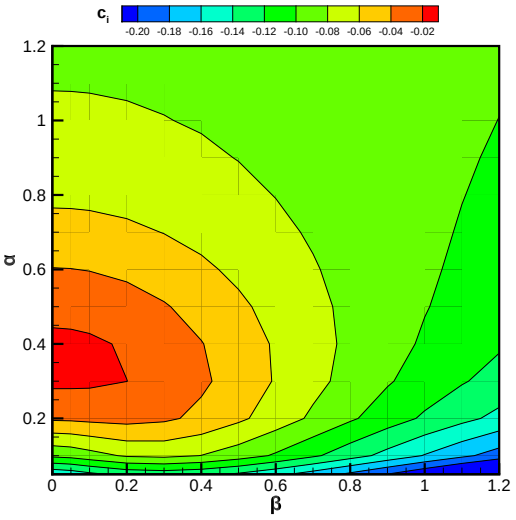

(a)

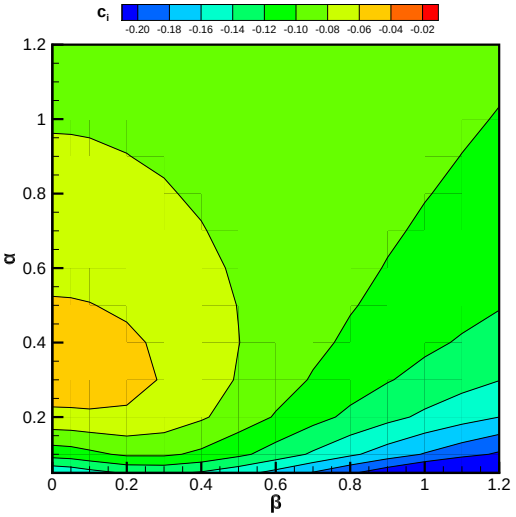

(b)

Figure 9: Contour plots of the temporally growth rate c_i for $s/s_{max} = 0.9$ (top) and $s/s_{max} = 0.95$ (bottom)

5 Conclusions

The algebraic stability of a PIV measured base flow evolving on the suction side of a low pressure turbine profile has been analyzed. A polynomial fitting of the experimental data has been developed in order to provide a base flow velocity profile suitable for the solution of the OSS eigenvalue problem. The Gaster's transformation has been adopted to convert the temporally growth rate into spatial growth rate for the less stable eigenvalue on the OSS discrete spectrum. However, it can only be applied in the range of wavenumbers that leads to a close to zero temporally growth rate (i.e. close to the neutral curve).

The investigated base flow results stable with respect to algebraic growing mechanism even though the measurements indicates that a laminar to turbulent transition occurs in the late part of the flow domain. It is argued that, due to the strong free stream turbulence, the boundary layer should follow a non-modal growing disturbance which leads to the formation of streaks that are indeed observed in the flow.

References

Andersson P, Berggren M, Henningson DS (1999) Optimal disturbances and bypass transition in boundary layers. Physics of Fluids (1994-present) 11(1):134–150

Arnal D (1994) Boundary layer transition: predictions based on linear theory. In: In AGARD, Special Course on Progress in Transition Modelling 63 p (SEE N94-33884 10-34), vol 1

Gaster M (1962) A note on the relation between temporally-increasing and spatially-increasing disturbances in hydrodynamic stability. Journal of Fluid Mechanics 14(02):222–224

Lengani D, Simoni D (2015) Recognition of coherent structures in the boundary layer of a low-pressure-turbine blade for different free-stream turbulence intensity levels. International Journal of Heat and Fluid Flow 54:1–13

Morkovin MV (1969) On the many faces of transition. In: Viscous drag reduction, Springer, pp 1–31

Schmid PJ, Henningson DS (2012) Stability and transition in shear flows, vol 142. Springer Science & Business Media

Smith A, Gamberoni N (1956) Transition, pressure gradient and stability theory. rep. no. es 26388, douglas aircraft co